This paper is published as part of a *PCCP* themed issue on dynamic nuclear polarization

Guest Editors: Robert Griffin and Thomas Prisner

Editorials

High field dynamic nuclear polarization—the renaissance
R. G. Griffin and T. F. Prisner, *Phys. Chem. Chem. Phys.*, 2010, **12**, 5737
http://dx.doi.org/10.1039/c0cp90019b

The discovery and demonstration of dynamic nuclear polarization—a personal and historical account
Charles P. Slichter, *Phys. Chem. Chem. Phys.*, 2010, **12**, 5741
http://dx.doi.org/10.1039/c003286g

Communications

High power pulsed dynamic nuclear polarisation at 94 GHz
Robert I. Hunter, Paul A. S. Cruickshank, David R. Bolton, Peter C. Riedi and Graham M. Smith, *Phys. Chem. Chem. Phys.*, 2010, **12**, 5752
http://dx.doi.org/10.1039/c002251a

Papers

DNP enhanced NMR using a high-power 94 GHz microwave source: a study of the TEMPOL radical in toluene
Eugeny V. Kryukov, Mark E. Newton, Kevin J. Pike, David R. Bolton, Radoslaw M. Kowalczyk, Andrew P. Howes, Mark E. Smith and Ray Dupree, *Phys. Chem. Chem. Phys.*, 2010, **12**, 5757
http://dx.doi.org/10.1039/c003189e

Rapid sample injection for hyperpolarized NMR spectroscopy
Sean Bowen and Christian Hilty, *Phys. Chem. Chem. Phys.*, 2010, **12**, 5766
http://dx.doi.org/10.1039/c002316g

Slice-selective single scan proton COSY with dynamic nuclear polarisation
Rafal Panek, Josef Granwehr, James Leggett and Walter Köckenberger, *Phys. Chem. Chem. Phys.*, 2010, **12**, 5771
http://dx.doi.org/10.1039/c002710n

Prospects for sub-micron solid state nuclear magnetic resonance imaging with low-temperature dynamic nuclear polarization
Kent R. Thurber and Robert Tycko, *Phys. Chem. Chem. Phys.*, 2010, **12**, 5779
http://dx.doi.org/10.1039/c0cp00157k

Liquid state DNP using a 260 GHz high power gyrotron
Vasyl Denysenkov, Mark J. Prandolini, Marat Gafurov, Deniz Sezer, Burkhard Endeward and Thomas F. Prisner, *Phys. Chem. Chem. Phys.*, 2010, **12**, 5786
http://dx.doi.org/10.1039/c003697h

Exploring the limits of electron-nuclear polarization transfer efficiency in three-spin systems
Nikolas Pomplun and Steffen J. Glaser, *Phys. Chem. Chem. Phys.*, 2010, **12**, 5791
http://dx.doi.org/10.1039/c003751f

Dynamic nuclear polarization experiments at 14.1 T for solid-state NMR
Yoh Matsuki, Hiroki Takahashi, Keisuke Ueda, Toshitaka Idehara, Isamu Ogawa, Mitsuru Toda, Hideo Akutsu and Toshimichi Fujiwara, *Phys. Chem. Chem. Phys.*, 2010, **12**, 5799
http://dx.doi.org/10.1039/c002268c

Trityl biradicals and ^{13}C dynamic nuclear polarization
Sven Macholl, Haukur Jóhannesson and Jan Henrik Ardenkjaer-Larsen, *Phys. Chem. Chem. Phys.*, 2010, **12**, 5804
http://dx.doi.org/10.1039/c002699a

Feasibility of *in vivo* ^{15}N MRS detection of hyperpolarized ^{15}N labeled choline in rats
Cristina Cudalbu, Arnaud Comment, Fiodar Kurdzesau, Ruud B. van Heeswijk, Kai Uffmann, Sami Jannin, Vladimir Denisov, Deniz Kirik and Rolf Gruetter, *Phys. Chem. Chem. Phys.*, 2010, **12**, 5818
http://dx.doi.org/10.1039/c002309b

Polychlorinated trityl radicals for dynamic nuclear polarization: the role of chlorine nuclei
Juan Carlos Paniagua, Verónica Mugnaini, Cristina Gabellieri, Miguel Feliz, Nans Roques, Jaume Veciana and Miquel Pons, *Phys. Chem. Chem. Phys.*, 2010, **12**, 5824
http://dx.doi.org/10.1039/c003291n

Shuttle DNP spectrometer with a two-center magnet
Alexander Krahn, Philip Lottmann, Thorsten Marquardsen, Andreas Tavernier, Maria-Teresa Türke, Marcel Reese, Andrei Leonov, Marina Bennati, Peter Hoefer, Frank Engelke and Christian Griesinger, *Phys. Chem. Chem. Phys.*, 2010, **12**, 5830
http://dx.doi.org/10.1039/c003381b

Properties of dinitroxides for use in dynamic nuclear polarization (DNP)
Cédric Ysacco, Egon Rizzato, Marie-Alice Virolleaud, Hakim Karoui, Antal Rockenbauer, François Le Moigne, Didier Siri, Olivier Ouari, Robert G. Griffin and Paul Tordo, *Phys. Chem. Chem. Phys.*, 2010, **12**, 5841
http://dx.doi.org/10.1039/c002591g

Pushing the limit of liquid-state dynamic nuclear polarization at high field
J. A. Villanueva-Garibay, G. Annino, P. J. M. van Bentum and A. P. M. Kentgens, *Phys. Chem. Chem. Phys.*, 2010, **12**, 5846
http://dx.doi.org/10.1039/c002554m

Solid-state dynamic nuclear polarization at 263 GHz: spectrometer design and experimental results
Melanie Rosay, Leo Tometich, Shane Pawsey, Reto Bader, Robert Schauwecker, Monica Blank, Philipp M. Borchard, Stephen R. Cauffman, Kevin L. Felch, Ralph T. Weber, Richard J. Temkin, Robert G. Griffin and Werner E. Maas, *Phys. Chem. Chem. Phys.*, 2010, **12**, 5850
http://dx.doi.org/10.1039/c003685b

Resolution and polarization distribution in cryogenic DNP/MAS experiments
Alexander B. Barnes, Björn Corzilius, Melody L. Mak-Jurkauskas, Loren B. Andreas, Vikram S. Bajaj, Yoh Matsuki, Marina L. Belenky, Johan Lugtenburg, Jagadishwar R. Sirigiri, Richard J. Temkin, Judith Herzfeld and Robert G. Griffin, *Phys. Chem. Chem. Phys.*, 2010, **12**, 5861
http://dx.doi.org/10.1039/c003763j

Application of *ex situ* dynamic nuclear polarization in studying small molecules
Christian Ludwig, Ildefonso Marin-Montesinos, Martin G. Saunders, Abdul-Hamid Emwas, Zoe Pikramenou, Stephen P. Hammond and Ulrich L. Günther, *Phys. Chem. Chem. Phys.*, 2010, **12**, 5868
http://dx.doi.org/10.1039/c002700f

^{2}H-DNP-enhanced ^{2}H–^{13}C solid-state NMR correlation spectroscopy
Thorsten Maly, Loren B. Andreas, Albert A. Smith and Robert G. Griffin, *Phys. Chem. Chem. Phys.*, 2010, **12**, 5872
http://dx.doi.org/10.1039/c003705b

Thermoresponsive, spin-labeled hydrogels as separable DNP polarizing agents
Björn C. Dollmann, Matthias J. N. Junk, Michelle Drechsler, Hans W. Spiess, Dariush Hinderberger and Kerstin Münnemann, *Phys. Chem. Chem. Phys.*, 2010, **12**, 5879
http://dx.doi.org/10.1039/c003349a

A dedicated spectrometer for dissolution DNP-NMR spectroscopy
James Leggett, Robert Hunter, Josef Granwehr, Rafal Panek, Angel J. Perez-Linde, Anthony J. Horsewill, Jonathan McMaster, Graham Smith and Walter Köckenberger, *Phys. Chem. Chem. Phys.*, 2010, **12**, 5883
http://dx.doi.org/10.1039/c002566f

Optimization of dynamic nuclear polarization experiments in aqueous solution at 15 MHz/9.7 GHz: a comparative study with DNP at 140 MHz/94 GHz
Maria-Teresa Türke, Igor Tkach, Marcel Reese, Peter Höfer and Marina Bennati, *Phys. Chem. Chem. Phys.*, 2010, **12**, 5893
http://dx.doi.org/10.1039/c002814m

Water ^{1}H relaxation dispersion analysis on a nitroxide radical provides information on the maximal signal enhancement in Overhauser dynamic nuclear polarization experiments
Marina Bennati, Claudio Luchinat, Giacomo Parigi and Maria-Teresa Türke, *Phys. Chem. Chem. Phys.*, 2010, **12**, 5902
http://dx.doi.org/10.1039/c002304n

Dynamic nuclear polarization-enhanced solid-state NMR spectroscopy of GNNQQNY nanocrystals and amyloid fibrils
Galia T. Debelouchina, Marvin J. Bayro, Patrick C. A. van der Wel, Marc A. Caporini, Alexander B. Barnes, Melanie Rosay, Werner E. Maas and Robert G. Griffin, *Phys. Chem. Chem. Phys.*, 2010, **12**, 5911
http://dx.doi.org/10.1039/c003661g

A 200 GHz dynamic nuclear polarization spectrometer
Brandon D. Armstrong, Devin T. Edwards, Richard J. Wylde, Shamon A. Walker and Songi Han, *Phys. Chem. Chem. Phys.*, 2010, **12**, 5920
http://dx.doi.org/10.1039/c002290j

Liquid state DNP using a 260 GHz high power gyrotron

Vasyl Denysenkov, Mark J. Prandolini, Marat Gafurov, Deniz Sezer, Burkhard Endeward and Thomas F. Prisner*

Received 26th February 2010, Accepted 27th April 2010
First published as an Advance Article on the web 11th May 2010
DOI: 10.1039/c003697h

Dynamic nuclear polarization (DNP) at high magnetic fields (9.2 T, 400 MHz ^{1}H NMR frequency) requires high microwave power sources to achieve saturation of the EPR transitions. Here we describe the first high-field liquid-state DNP results using a high-power gyrotron microwave source (20 W at 260 GHz). A DNP enhancement of −29 on water protons was obtained for an aqueous solution of Fremy's Salt; in comparison the previous highest value was −10 using a solid-state microwave power source (maximum power 45 mW). The increased enhancements are partly due to larger microwave saturation and elevated sample temperature. These experimentally observed DNP enhancements, which by far exceed the predicted values extrapolated from low-field DNP experiments, demonstrate experimentally that DNP is possible in the liquid state also at high magnetic fields.

Introduction

Dynamic nuclear polarization (DNP) is an important technique to enhance NMR signals. Griffin[1] and Golman[2] showed with their pioneering work that very high DNP enhancements could be obtained in solids also at high magnetic fields. These substantial signal-to-noise enhancements have been used in solid state magic angle sample spinning experiments on biomolecules[3] or in the liquid state, after fast liquefaction of the sample, either by rapid dissolution of the pellet in hot solvent[4] or by laser melting.[5] This work triggered new initiatives investigating the possibility of directly achieving Overhauser DNP polarization at high magnetic fields in the liquid phase, avoiding freeze-thaw cycling of the sample. One approach is to polarize the liquid sample at low magnetic fields, followed by a fast shuttle for high-field NMR detection.[6] In this case, large initial enhancements can be obtained, however losses due to the shuttle time, the Boltzmann factor and magnetic field profile along the shuttle path between polarization and detection fields limit the final reachable signal enhancement.[7]

Our approach is to polarize the nuclear spins directly at the magnetic field of the NMR detection,[8] similar to the classic approach at lower magnetic fields.[9] This *in situ* approach has the advantage that nuclear and electron spins can be excited and detected simultaneously and no physical change of the sample is necessary. Disadvantages for liquid samples are high microwave (MW) absorption of the sample, especially for water based solvents, and the lower expected enhancements that can be achieved *via* the Overhauser effect at high magnetic fields. The reason for this is that the Overhauser effect is driven by electron-nuclear cross relaxation processes, which become inefficient at high electron Larmor frequency compared to the electron spin relaxation processes. Recently we and others showed that enhancements at high magnetic fields are substantially higher than expected from extrapolations of low-field DNP results.[10,11] In these experiments the DNP enhancement was limited by the available MW power of solid-state microwave sources. In this paper we describe the implementation of a 260 GHz gyrotron oscillator (GYCOM, Russia) to our liquid-state 400 MHz DNP spectrometer and demonstrate our first experimental DNP enhancements obtained with this MW source on an aqueous solution of Fremy's Salt.

Institute of Physical and Theoretical Chemistry and Center of Biomolecular Magnetic Resonance, Goethe University Frankfurt, Germany. E-mail: Prisner@chemie.uni-frankfurt.de

Results and discussion

Fig. 1 compares our DNP experiments of a liquid solution of Fremy's Salt in water using a high (20 W gyrotron) or low (45 mW solid-state source) MW power source. In both cases the low field ^{15}N hyperfine EPR transition was pumped continuously, while the NMR free induction decay (FID) of the water protons and corresponding Fourier transformation (FT) have been recorded (dots). The NMR pulse repetition time was 4 s and 16 FID signals were averaged in all cases. The NMR reference spectrum without MW pumping is shown in black. The experimental DNP enhancement is calculated by $\varepsilon = ({I_{\mathrm{NMR}}}^{\mathrm{MW}} - I_{\mathrm{NMR}})/I_{\mathrm{NMR}}$, where ${I_{\mathrm{NMR}}}^{\mathrm{MW}}$ and I_{NMR} are the integrated NMR signal intensities with and without MW, respectively.

The line shape distortions of the NMR lines without MW excitation result from static magnetic field inhomogeneity introduced by the MW waveguide close to the sample (see below). The additional distortions and line shift of the NMR lines with MW irradiation result from sample heating and inhomogeneity of the MW field strength along the sample capillary. For the experiments shown in Fig. 1(a) the full power of the gyrotron (20 W) had to be substantially attenuated to limit the sample heating to approximately 35 °C (sample temperature of 60 °C). If we extrapolate from a calibration curve measuring MW power against water-proton

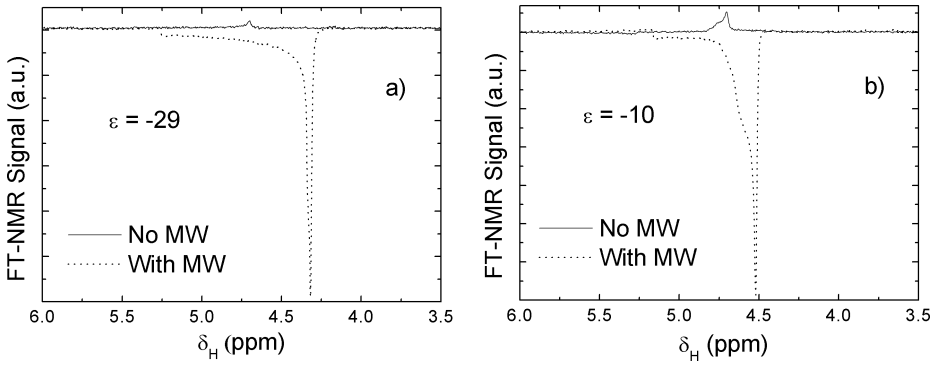

Fig. 1 Water ^{1}H NMR spectra with MW (dots) and without MW (solid) on 40 mM aqueous Fremy's Salt solutions with (a) using a high power gyrotron, and (b) a low power solid-state MW source.

NMR shift for 0.03 mm capillaries, we can estimate the power at the cavity to be approximately 110 mW. This MW power corresponds to a MW magnetic field strength of $B_{MW} = 1.5$ G at the sample. At this MW power a DNP enhancement of −29 was observed. For comparison, Fig. 1(b) shows DNP experiment on a 40 mM Fremy's Salt solution under similar conditions using the maximum power of the solid-state MW source (25 mW at the cavity, $B_{MW} = 0.7$ G). In this case a DNP enhancement of −10 at a temperature of 40 °C was achieved, the sample being placed in a 0.05 mm i.d. capillary.[10] The leakage factor in both cases was measured to be $f = 0.94$.

The Overhauser DNP signal enhancement factor ε for liquid samples can be written as:[9]

$$\varepsilon = \xi f s \frac{\gamma_e}{\gamma_p}$$

where γ_e and γ_p are the electronic and nuclear spin magnetogyric ratios, ξ is the coupling factor, s is the saturation factor and $f = 1 - T_{1R}/T_{1W}$ is the leakage factor. T_{1R} and T_{1W} are the nuclear spin relaxation times with (R) and without (W) radicals, respectively. In our case the nuclear spin is the proton spin of the water solvent and therefore the ratio γ_S/γ_p is 660. While ε and f are easily determined experimentally, the saturation factor s is much more difficult to obtain for nitroxides at high magnetic fields by EPR measurements. This is due to the very short longitudinal and transversal relaxation times of the nitroxide electron spin in liquid solution (<200 ns)[8,10] and polarization transfer between the nitrogen spin hyperfine lines by Heisenberg spin exchange and nitrogen nuclear spin relaxation. For a single homogeneous EPR line, the inverse saturation factor $1/s$ depends linearly on the inverse microwave power $1/P_{MW}$. This has been used in the past to predict DNP enhancements ε_{max} under saturation condition ($s = 1$). Under our experimental conditions the situation is more complex: the sample is heated due to MW absorption, leading to higher sample temperature as well as changed relaxation times and coupling factor as a function of MW power. Thus a 3 times higher enhancement observed with our gyrotron source might have its origin in a changed saturation and/or coupling factor.

In a previous paper,[12] we have shown that the saturation factor s for nitroxide radicals can be quantitatively calculated based on the Redfield perturbation theory, including the effects of nitrogen relaxation and Heisenberg exchange. Most of the parameters needed for this calculation, like homogeneous EPR linewidth and Heisenberg exchange rate, can be measured using EPR spectroscopy. However, as explained above a direct determination of T_{1e} in aqueous solutions of nitroxides at high field is difficult. While T_{1e} has been measured for aqueous TEMPONE solutions at EPR frequencies up to 95 GHz[13] and estimates have been given for TEMPOL at 260 GHz,[10] T_{1e} of Fremy's Salt has so far only been determined at low fields (X-Band, 9 GHz) to be 380 ns.[14] Assuming two homogeneous hyperfine lines without nuclear spin flips and Heisenberg exchange the saturation factor s can be calculated for different T_{1e} values, taking the MW field strength B_1 from the pulsed EPR experiment (see Experimental section), the transversal relaxation time and the hyperfine splitting from the EPR spectra, which are in good agreement with X-band measurements.[15] For T_{1e} values in the range of 100–400 ns the saturation s changes between high and low MW power only by a ratio s(110 mW)/s(25 mW) of 2.2–1.3. Heisenberg spin exchange and nuclear spin relaxation will further lower this ratio; therefore the observed strong increase of the DNP enhancement cannot be explained by only the saturation factor itself.

In a recent publication we were able to show that it is possible to calculate dipolar correlations functions for radical-solvent pairs from molecular dynamics studies.[16] In the case of TEMPOL in water a coupling factor ξ in very good agreement with our low-power experimental DNP results could be achieved. In contrast, high-field coupling factors predicted from low-field DNP experiments assuming a simple translational and rotational motion model between electron and nuclear spin[9,17] have been too low. The MD study showed that additional high frequency modes, other than translational and rotational diffusion, contribute to the spectral density. MD calculations performed for Fremy's Salt radicals in aqueous solutions at temperatures of 25, 35, 45 °C are shown in Fig. 2.

There is a strong dependence of the coupling factor ξ on the temperature T. Extrapolating the coupling factor to 60 °C, where the high-power DNP experiment was performed leads to an increase of the coupling factor of 1.5–2 going from 40 to 60 °C. This is again smaller than the experimentally observed increase of the DNP enhancement. Therefore we can

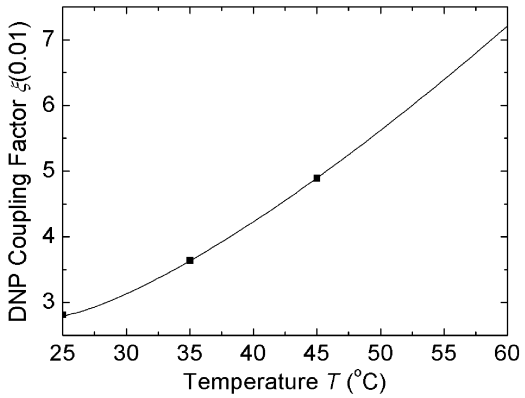

Fig. 2 Coupling factors ξ calculated from MD simulations of Fremy's Salt in water for 25, 35 and 45 °C. The dotted line shows a fit with $\xi(T) = 0.028 + 0.039 \times (T - 25\ ^{\circ}C)^{1.33}$ to the calculated values to extrapolate ξ at 60 °C.

conclude that the high enhancements observed with the gyrotron MW source is a combination of the increased saturation of the ^{15}N Fremy's Salt nitroxide and an increased coupling factor ξ by MW sample heating.

The coupling factor at 60 °C of $\xi = 0.072$ extrapolated from MD calculations and the DNP enhancement of −29 implies that the saturation achieved with the 110 mW power is 0.65. This value is higher than the saturation calculated above, s(110 mW) = 0.3–0.5 depending on T_{1e} and shows significant contribution of Heisenberg exchange to the saturation of the electron spin system. The projected coupling factor of 0.072 at 60 °C would correspond to a maximum enhancement of $\varepsilon_{max} = -45$ at full ERP saturation ($s = 1$).

Experimental

The DNP experiments were performed with ^{15}N Fremy's Salt $K_2(SO_3)_2NO$ (di-potassium nitrosyl-disulfonate), in a 50 mM K_2CO_3 buffer solution to reduce the decomposition rate.

Radical concentration was determined by X-band EPR measurements, proton NMR relaxation measurements, and optically. A 40 mM Fremy's Salt solution was placed in a quartz capillary with 0.03 mm i.d. in order to reduce the heating effects from the high power gyrotron source as much as possible.

Our home-built 260 GHz liquid-state DNP spectrometer equipped with a low MW power source is described in detail in ref. 8. The spectrometer is designed for *in situ* DNP, NMR, and EPR experiments, where continuous wave MW excitation and radio frequency (RF) pulses can be applied simultaneously. In this setup a standard 400 MHz Bruker NMR spectrometer was modified to include a continuous wave EPR bridge based on metallodielectric waveguide technology. The MW bridge consists of a solid-state MW source (VDI, USA) with a maximum output power of 45 mW, which is frequency tunable within the range of 256–263 GHz; an interferometer reference arm; a frequency counter; and an EPR signal detection channel. The total transmission system losses are less than 2 dB resulting in about 25 mW continuous MW power at the sample position. The heart of the DNP spectrometer is a double resonance structure for aqueous samples, consisting of a helix which serves as a NMR coil for excitation and detection as well as a cylindrical TE_{011} cavity for EPR. The MW cavity has two important features: first, it drastically reduces the MW electrical field strength at the sample position, thus avoiding excessive heating of the liquid sample; and second, it enhances the MW magnetic field strength at the sample position. The maximum temperature increase for pure water using maximum power from the solid-state MW source depends on the diameter of the capillary containing the sample: for samples with 0.03 mm and 0.05 mm i.d., a temperature increase of 8 and 21 °C, respectively, was observed by measuring the shift of the water proton NMR at maximum power of the solid state source. The magnetic field inhomogeneity caused by the metallodielectic waveguide results in a broad NMR peak with a total line width of 130 Hz. The DNP active sample volume is 3–4 nL for 0.05 mm capillaries. The conversion factor for the helix from MW power P_{MW} to field strength B_{MW} has been determined by a single pulse EPR FID experiment on a fluoranthenyl hexafluorophosphate ($(FA)_2PF_6$) single crystal using a 200 mW orotron source (GYCOM, Russia). The amplitude and shape of the FID signal were monitored as a function of the applied pulse length. Optimal $\pi/2$ and π pulses were estimated to be 80 ns and 160 ns long, respectively. This leads to a MW field amplitude of $B_{MW} = 1.2$ G in this case. The Q-factor of the helix probe loaded with the fluoranthenyl single crystal was 1.5 times smaller compared to aqueous samples due to distortions of the microwave field introduced by the irregular shape of the crystal. Therefore the maximum MW field strength with the solid-state source used for the DNP experiments can be calculated to be $B_{MW} = 0.7$ G.

This initial DNP setup has been modified to include a high-power gyrotron MW source. A quasioptical MW transmission line connects the gyrotron power source to the liquid-state (LS) DNP spectrometer used for these experiments and a solid-state (SS) MAS DNP spectrometer both operating at 9.2 T, corresponding to 400 MHz ^1H NMR frequency and 260 GHz EPR frequency (Fig. 3). The transmission line consists of 18 mm i.d. corrugated waveguide pieces with a total length of 14 m, and some passive components such as calorimeter, attenuator, 90° bends, and mechanical MW switch. Total MW losses are measured to be 3 dB to the SS MAS DNP spectrometer, and 4 dB to the LS DNP spectrometer.

The gyrotron is inherently a single frequency oscillator operating in a magnetic field of 4.7 T provided by a cryomagnet. The operation frequency of the gyrotron is close to the second harmonic of the electron's cyclotron resonance and is determined by the "non-tunable" cavity of the gyrotron equal to 258.9 GHz. It can be slightly tuned by changing the temperature of the cooling water for the copper gyrotron resonator. A temperature change between 15–35 °C changes the gyrotron resonance frequency by about 60 MHz. For frequency stabilization a P-307 cooler (TermoTek AG, Germany) with a temperature stability ±0.1 K has been used. The gyrotron frequency was calibrated with our liquid state DNP spectrometer by simultaneous measurement of the EPR spectra of TEMPOL by sweeping the magnetic field of the LS DNP spectrometer with calibration of the main field

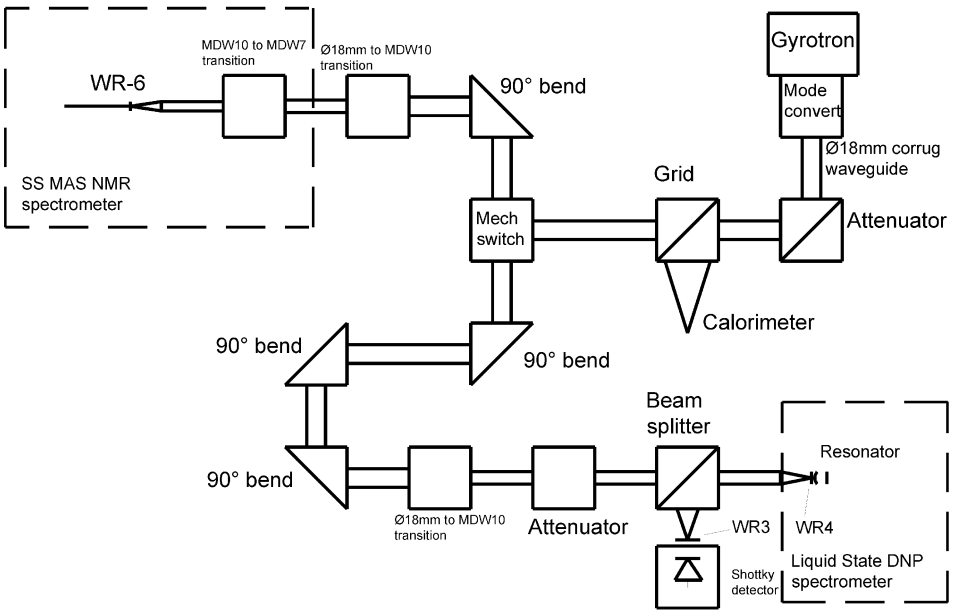

Fig. 3 Block-diagram of the DNP setup. The parts in the dashed lines belong to the two DNP spectrometers; the other parts belong to the transmission line connecting the gyrotron source to the spectrometers.

by measurement of the water proton NMR frequency. The frequency stability of the gyrotron has been evaluated with an EPR signal of a TEMPOL solution monitored for 1 h by periodic sweeping of the magnetic field of the LS DNP spectrometer. From such consecutive EPR spectra the gyrotron frequency drift was estimated to be in the range of 6×10^{-6} h^{-1}. This is stable enough to run DNP experiments on liquid Fremy's Salt solutions, which show the narrowest EPR lines among nitroxides at high fields.

Description of molecular dynamic simulations for Fremy's Salt

Molecular dynamics simulations of Fremy's Salt in water were performed for three different temperatures: 298, 308 and 318 K. The simulation and analysis approach first introduced in ref. 16 were followed in the present study. In summary, one molecule of Fremy's Salt and two potassium counter ions were placed in a cubical box initially containing 3000 water molecules at the experimental water density for the appropriate temperature. After deleting eight waters overlapping with the Fremy's Salt molecule and replacing two waters with ions, 2990 waters were left. The simulations were performed with the simulation package NAMD[18] and the CHARMM force field[19] under constant temperature and volume using periodic boundary conditions. As discussed in detail in ref. 16, different values were used for the friction coefficient of the Langevin thermostat at different temperatures such that the resulting translational diffusion of the employed TIP3P[20] water model matched the experimental values for bulk water. An integration time step of 2 fs was employed and the simulations for each temperature lasted for 2.1 ns. Coordinates were saved for subsequent analysis every 75 integration steps (0.15 ps) and the first 600 snapshots (90 ps) were excluded from the analysis.

Electron spin-nuclear spin dipolar correlation functions were calculated from the MD trajectories using the positions of the oxygen and nitrogen atoms of the nitroxide moiety and the water protons as explained in ref. 16. To calculate the coupling factors reported in Fig. 2, the dipolar correlation functions were fitted to a sum of three exponential decays. Their long-time tail was separately fitted to power-law decay with exponent of $-3/2$ (see ref. 16 for more details.) Note that any possible contribution due to scalar coupling between the electron and nuclear spins has been ignored in the present analysis. However, quantum mechanical calculations reported in ref. 16 indicate that the DNP contribution of the scalar coupling between water protons and the unpaired nitroxide electron is at most a few percent of the dipolar contribution. Nevertheless, if present, such scalar coupling can only reduce the absolute value of the calculated dipolar coupling factors, implying a somewhat larger degree of saturation than presently estimated without changing the conclusions of this study.

Conclusion

Liquid state DNP at high magnetic fields has to fulfil two important experimental requirements: on the one hand, to achieve a high MW magnetic field strength at the sample to saturate the electron transitions of the radical and on the other hand, to avoid heating of the sample by the MW electrical field component. Therefore a resonant MW structure to separate electrical and magnetic field components has to be used, at least for lossy solvents like water. The use of such MW resonant structures additionally increases the magnetic field strength at the sample significantly. Therefore reasonable DNP enhancements can be obtained already with low power solid state MW sources. Nevertheless, in such cases only single mode resonators can be used, which exhibit large conversion

factors but severely limit the size of the sample. Double resonance structures with larger sample volumes often have much lower MW conversion factors and therefore need more powerful MW sources to obtain maximum enhancement. Gyrotrons have been exploited for solid state DNP experiments[21–23] and are available in the frequency range of 100–1000 GHz matching well the modern high-resolution NMR spectrometers.

Here we have shown that with a 20 W gyrotron source operating at 260 GHz liquid state DNP enhancement for water protons of −29 has been achieved at a ^{1}H frequency of 400 MHz and a magnetic field of 9.2 T. The observed higher enhancement is mainly a result of better saturation of the electron spin transition; additionally the elevated temperature leads also to a somewhat larger coupling factor. Presently, we are working on new double resonance structures that have much larger sample volumes and better field homogeneity to improve the overall NMR sensitivity and a possibility to stabilize sample temperature by active cooling. This will allow accurate experimental determination of the coupling factor and its temperature dependence. The observed enhancements are by far larger than expected from theoretical models based on translational and rotational diffusion of the DNP agent and target molecular pair and promising for applications in liquids at high magnetic fields. To understand the physical origin of this unexpected large enhancements will be a prerequisite for further optimization of the liquid DNP effect at high magnetic fields and potential applications.

Acknowledgements

Bernhard Thiem and Jens Törring are thanked for the construction of the magnetic field sweep system. We thank Domink Margraf for the synthesis of the Fremy's Salt. The one-dimensional organic conductor fluoranthenyl hexafluorophosphate ($(FA)_2PF_6$) single crystal is a gift from Prof. Dormann from the University Karlsruhe. Frank Engelke, Alexander Krahn and Thorsten Marquardsen are thanked for their help in the construction of the high-field DNP probe. We thank Lenica Reggie and Prof. Clemens Glaubitz for planning and implementation of the gyrotron source, and Vladimir Zapevalov from Gycom for the design, construction and testing of the DNP-gyrotron. We are grateful to Sevdalina Lyubenova and Jan Krummenacker for fruitful discussions of obtained results. This project was funded by the framework 6 EU Design Study Project *Bio-DNP*. The gyrotron source was funded by the Center of Excellence Frankfurt *Macromolecular complexes*.

References

1 L. R. Becerra, G. J. Gerfen, R. J. Temkin, D. J. Singel and R. G. Griffin, *Phys. Rev. Lett.*, 1993, **71**, 3561–3564.
2 J. Ardenkjaer-Larsen, B. Fridlund, A. Gram, G. Hansson, L. Hansson, M. Lerche, R. Servin, M. Thaning and K. Golman, *Proc. Natl. Acad. Sci. U. S. A.*, 2003, **100**, 10158–10163.
3 T. Maly, G. T. Debelouchina, V. S. Bajaj, K.-N. Hu, C.-G. Joo, M. L. Mak-Jurkauskas, J. R. Sirigiri, P. C. A. van der Wel, J. Herzfeld, R. J. Temkin and R. G. Griffin, *J. Chem. Phys.*, 2008, **128**, 052211(1-19).
4 K. Golman, R. I. Zandt, M. Lerche, R. Pehrson and J. H. Ardenkjaer-Larson, *Cancer Res.*, 2006, **66**, 10855–10860.
5 C.-G. Joo, K.-N. Hu, J. A. Bryant and R. G. Griffin, *J. Am. Chem. Soc.*, 2006, **128**, 9428–9432.
6 M. Reese, D. Lennartz, T. Marquardsen, P. Höfer, A. Tavernier, P. Carl, T. Schippmann, M. Bennati, T. Carlomagno, F. Engelke and C. Griesinger, *Appl. Magn. Reson.*, 2008, **34**, 301–311.
7 M. Reese, M.-T. Türke, I. Tkach, G. Parigi, C. Luchinat, T. Marquardsen, A. Tavernier, P. Höfer, F. Engelke, C. Griesinger and M. Bennati, *J. Am. Chem. Soc.*, 2009, **131**, 15086–15087.
8 V. P. Denysenkov, M. J. Prandolini, A. Krahn, M. Gafurov, B. Endeward and T. F. Prisner, *Appl. Magn. Reson.*, 2008, **34**, 289–299.
9 K. N. Hausser and D. Stehlik, *Advan. Magn. Res.*, 1968, **3**, 79–139.
10 M. J. Prandolini, V. P. Denysenkov, M. Gafurov, B. Endeward and T. F. Prisner, *J. Am. Chem. Soc.*, 2009, **131**, 6090–6092.
11 P. Hoefer, G. Parigi, C. Luchinat, P. Carl, G. Guthausen, M. Reese, T. Carlomagno, Ch. Griesinger and M. Bennati, *J. Am. Chem. Soc.*, 2008, **130**, 3254–3255.
12 D. Sezer, M. Gafurov, M. J. Prandolini, V. P. Denysenkov and T. F. Prisner, *Phys. Chem. Chem. Phys.*, 2009, **11**, 6638–6653.
13 W. Froncisz, T. G. Camenisch, J. J. Ratke, J. R. Anderson, W. K. Subczynski, R. A. Strangeway, J. W. Sidabras and J. S. Hyde, *J. Magn. Reson.*, 2008, **193**, 297–304.
14 M. Dutka, R. J. Gurbiel, J. Koziol and W. Froncisz, *J. Magn. Reson.*, 2004, **170**, 220–227.
15 S. A. Goldman, G. V. Bruno, C. F. Polnaszek and J. H. Freed, *J. Chem. Phys.*, 1972, **56**, 716–736.
16 D. Sezer, M. J. Prandolini and T. F. Prisner, *Phys. Chem. Chem. Phys.*, 2009, **11**, 6626–6637.
17 B. D. Armstrong, M. D. Lingwood, E. R. McCarney, P. Brown, P. Bluemler and S. Han, *J. Magn. Reson.*, 2008, **191**, 273–281.
18 J. J. Phillips, R. Braun, W. Wang, J. Gumbart, E. Tajkorshit, E. Villa, C. Chipot, R. D. Skeel, L. Kale and K. Schulten, *J. Comput. Chem.*, 2005, **26**, 1781–1802.
19 A. D. MacKerell, D. Bashford, M. Bellott, R. Dunbrack, E. Evanseck, M. Field, S. Fischer, J. Gao, H. Guo, S. Ha, D. Joseph-McCarthy, L. Kuchnir, K. Kuczera, F. T. K. Lau, C. Mattos, S. Michnick, T. Ngo, D. T. Nguyen, B. Prodhom, W. E. Reiher, B. Roux, M. Schlenkrich, J. C. Smith, R. Stote, J. Straub, M. Watanabe, J. Wiórkiewicz-Kuczera, D. Yin and M. Karplus, *J. Phys. Chem. B*, 1998, **102**, 3586–3616.
20 W. L. Jorgensen, J. Chandrasekhar, J. D. Madura, R. W. Impey and M. L. Klein, *J. Chem. Phys.*, 1983, **79**, 926–935.
21 V. S. Bajaj, M. K. Hornstein, K. E. Kreischer, J. R. Sirigiri, P. P. Woskov, M. L. Mak-Jurkauskas, J. Herzfeld, R. J. Temkin and R. G. Griffin, *J. Magn. Reson.*, 2007, **189**, 251–279.
22 T. Idehara, T. Saito, I. Ogawa, S. Mitsudo, Y. Tatematsu, M. H. La Agusu and S. Kobayashi, *Appl. Magn. Reson.*, 2008, **34**, 265–275.
23 V. Bratman, M. Glyavin, T. Idehara, Yu. Kalynov, A. Luchinin, V. Manuilov, S. Mitsudo, I. Ogawa, T. Saito, Y. Tatematsu and V. Zapevalov, *IEEE Trans. Plasma Sci.*, 2009, **37**, 36–43.

